Understanding the Magnetocatalytic Effect: Magnetism as a Driving Force for Surface Segregation

Donald J. Siegel,[1,*] Mark van Schilfgaarde,[2] and J. C. Hamilton[1]

[1]*Sandia National Laboratories, Mail Stop 9161, Livermore, California 94551, USA*

[2]*Chemical and Materials Engineering Department, Arizona State University, Tempe, Arizona 85287, USA*

(Received 28 July 2003; published 24 February 2004)

The magnetocatalytic (or Hedvall) effect refers to a change in the rate of a chemical reaction on a magnetic surface at the Curie point T_C. For Ni catalysts, experiments suggest the effect is related to a sudden increase in segregated surface C, a strong catalytic poison, at temperatures below T_C. However, the connection between magnetism and surface segregation is not understood. Using density functional theory and spin-dynamics simulations, we show that the solubility of C in Ni is significantly reduced in the ferromagnetic state, because C suppresses Ni magnetism and thereby increases the heat of solution. This explains the observed increase in C segregation and the reduced catalytic activity below T_C.

DOI: 10.1103/PhysRevLett.92.086101 PACS numbers: 68.35.Dv, 71.15.Mb, 75.70.–i, 82.65.+r

The magnetocatalytic effect (or Hedvall effect) refers to an abrupt change in the rate of a chemical reaction on a magnetic surface at the Curie point, T_C [1]. The explanation for this unexpected link between magnetism and chemistry has remained elusive since its discovery in 1934 [2]. Careful surface science experiments [3] on nickel have suggested that the effect could be caused by increased surface segregation of carbon [4–6], a catalytic poison, at temperatures below T_C. However, this explanation remains incomplete because the link between bulk magnetism and surface segregation of impurities is not understood. Here we establish this connection using *ab initio* calculations of the temperature-dependent solubility of carbon in nickel. Specifically, we show that the C solubility drops dramatically below T_C because C interstitials suppress Ni magnetism, an energetically unfavorable process. Below the Curie point, the nickel atoms can therefore regain their magnetism and lower their energy by driving carbon out of solution. We call this phenomenon *magnetoexpulsion* and note that it has been observed [7] and modeled [8] for hydrogen in nickel. This result has wide ranging implications since the solubility of impurities and interfacial segregation are key determinants of materials properties.

The Hedvall effect was first observed as a rapid increase in the decomposition rate of N_2O at temperatures above the Curie point of a Ni catalyst [2]. For the sake of simplicity, subsequent experiments [3,9] have studied the hydrogen-deuterium exchange reaction, $H_2 + D_2 \rightarrow 2HD$, thereby avoiding possible oxidation of the catalyst by the reactants. For example, Zeiger *et al.* [9] reported a sudden increase in the rate of HD production over a $Ni_{1-x}Cu_x$ catalyst at temperatures above T_C, and suggested that the effect was caused by a change in the electronic structure of the catalyst surface resulting from its change in magnetic state. This explanation was called into question by subsequent experiments [3], in which the same exchange reaction was studied over a Ni single crystal catalyst, showing that the Hedvall effect disappeared if C was completely removed from the catalyst. Since previous measurements had demonstrated reversible C surface segregation to Ni surfaces at temperatures below the Curie point [5], it was suggested [3,4] that the effect was due to catalyst poisoning by segregated C at temperatures below T_C. The poisoning effect was attributed to impurity blocking of catalytically active sites, a well known mechanism for catalyst deactivation [10–12]. Here we present electronic structure calculations demonstrating how bulk magnetism alters the segregation behavior of C on Ni surfaces. Combined with the aforementioned experimental results [3–5], these calculations provide a compelling model for how bulk magnetism can alter catalytic activity by inducing surface segregation.

This Letter describes two different calculations: In the first calculation we evaluate differences in heats of solution (and adsorption) for C impurities in paramagnetic and ferromagnetic nickel. This simplified model provides a qualitative understanding of enhanced carbon segregation on ferromagnetic Ni, based on carbon's effect on the magnetic moments of nearest-neighbor Ni atoms. In the second calculation, we describe a more quantitative model of the solubility of C in Ni as a function of temperature through the Curie point, which includes the dependence of the spin orientations on temperature. Previous measurements of C solubility in $Ni_{1-x}Co_x$ [13], measurements of H solubility in Ni [7], and a theoretical treatment of H in Ni [8] confirm our prediction of magnetoexpulsion of impurities below the Curie point, providing additional verification of our explanation for the magnetocatalytic effect.

Here we emphasize the effect of magnetism on the heat of solution, ΔH_{sol}, for carbon in nickel. The heat of segregation, ΔH_{seg}, is directly related to the heat of solution as follows:

$$\Delta H_{\mathrm{seg}} = \Delta H_{\mathrm{ads}} - \Delta H_{\mathrm{sol}}, \tag{1}$$

where ΔH_{ads} is the heat of adsorption. Magnetically induced changes in either ΔH_{ads} or ΔH_{sol} could alter ΔH_{seg} and, thus, the degree of surface segregation. Our calculations (see below) show a large dependence of ΔH_{sol} on the magnetic state and a smaller dependence of ΔH_{ads} on the magnetic state, implying that changes in ΔH_{seg} will be dominated by changes in ΔH_{sol}. This is a fortunate state of affairs since the Hedvall effect has been observed on polycrystalline surfaces with probable contamination. An explanation based primarily on magnetic changes in the bulk ΔH_{sol} can be applied more universally since it avoids the complicated effects of surface orientation and contamination on ΔH_{ads}.

Although ΔH_{seg} determines the equilibrium concentration of segregated C, diffusion rates determine how rapidly equilibrium is attained. Because C diffusion in Ni is slow at the Curie point, hysteresis effects in surface C coverage have been reported [5]. Carbon segregates slowly during cooling, and reenters the bulk more rapidly upon heating. These kinetic limitations can be estimated using the known diffusion rate, $D = 10^{-13}$ cm^2 s^{-1} at 350 °C [14], for C in Ni. For a time of $t = 1000$ s, corresponding to a temperature change of 5 °C in Hedvall's experiment [2], C diffuses over a distance of about 1000 Å. For a bulk C concentration of 100 ppm, this corresponds to a surface coverage of about 0.1 monolayer of C. For polycrystalline catalysts, C mobility will likely be further enhanced by rapid diffusion along grain boundaries. Since C coverages of much less than a monolayer are known to inhibit catalysis [3], we conclude that kinetic limitations exist, but do not prohibit observation of changes in catalytic activity due to C segregation.

We start by considering the magnetically induced change in the heat of solution for carbon in nickel, defined as $\delta\Delta H_{sol} = \Delta H_{sol}(\mathrm{FM}) - \Delta H_{sol}(\mathrm{PM})$, where FM denotes perfect collinear magnetic ordering (ferromagnetic) and PM denotes complete disordering (paramagnetic). Density functional [15] calculations based upon an all-electron linear muffin-tin orbital (LMTO) [16,17] method within the local [18] (spin) density approximation (LSDA) were performed on two different supercells, one containing 32 Ni atoms, and the other containing 32 Ni atoms and a single interstitial C atom in an octahedral site. We approximated paramagnetic Ni by calculating the relevant energies for nonmagnetic Ni. In the case of the supercell with carbon, the atomic positions and supercell volume were fully relaxed. The magnetically induced change in the heat of solution was evaluated according to

$$\delta\Delta H_{sol} = [E_{Ni}(\mathrm{PM}) - E_{Ni}(\mathrm{FM})] - [E_{Ni\text{-}C}(\mathrm{PM}) - E_{Ni\text{-}C}(\mathrm{FM})], \quad (2)$$

where the subscript Ni denotes the Ni supercell and Ni-C denotes the same supercell with an additional carbon atom. These calculations gave a magnetically induced change in the heat of solution, $\delta\Delta H_{sol} = 0.48$ eV/C, indicating that more energy is required to dissolve C in ferromagnetic Ni than in paramagnetic Ni. This implies that the solubility of carbon is less below the Curie point than it is above, precisely as required to cause increased carbon segregation below T_C. This change in the heat of solution is substantial, and is comparable in size to the Ni-C high temperature ($T \gg T_C$) ΔH_{sol} [13]. (Additional test calculations [19] verified that this result was not an artifact of our computational methodology, supercell size, etc.) Notably, our calculated $\delta\Delta H_{sol}$ is somewhat larger than what one might estimate by assuming the magnetic energy is local, in which case the magnetic energy cost for adding a C interstitial is $\approx 6 \times E_{mag} = 0.28$ eV. (Here $E_{mag} = 47$ meV is the calculated magnetization energy per Ni atom, and the factor of 6 accounts for the octahedral coordination of the C.)

Because of slow kinetics, an experimental measurement of ΔH_{sol} across T_C has, to our knowledge, not yet been reported for this system. However, the solubility of two related systems, NiCo-C [13] and Ni-H [7], has been examined over temperature ranges spanning their respective Curie points. In both cases a slight increase in ΔH_{sol} has been observed for $T < T_C$, thus supporting our prediction for Ni-C.

We turn now to a discussion of the electronic effects which link bulk magnetism and surface segregation. Figure 1 shows the partial density of states (DOS) and magnetic moments for bulk Ni atoms in successive shells around a C interstitial atom. Far from the carbon atom (bottom panel), the Ni DOS is virtually identical to that of pure Ni. As in bulk Ni, the nearly full d band is split by a standard Stoner mechanism into a full majority spin band and a partially filled minority band. The differing occupancy of the spin-up and spin-down bands is responsible for a magnetic moment of $\sim 0.6\mu_B$. For Ni atoms adjacent to C (see second panel from top), charge is transferred from Ni to the more electronegative C, shifting the minority band largely below the Fermi level. The magnetic moment of these Ni atoms is reduced to $\sim 0.2\mu_B$: C has largely quenched their magnetic moment. By coupling to the nonmagnetic interstitial C, the impetus for these sites to polarize through the Stoner mechanism is weakened. In the absence of C, Ni atoms lower their energy by aligning their magnetic moments. With C, the magnetic moments are quenched, thereby raising the energy of the system. The energy of ferromagnetic Ni is lowered by driving the C atoms out of solution (in this case to the surface), a process which we call magnetoexpulsion.

Previously, we justified our emphasis on the heat of solution by the claim that $\delta\Delta H_{sol} > \delta\Delta H_{ads}$. We evaluated $\delta\Delta H_{ads}$ by calculating the energy of relaxed Ni slabs with and without surface C in the paramagnetic and ferromagnetic states. We find that magnetically induced changes to ΔH_{ads} are indeed smaller than those for ΔH_{sol}, with $\delta\Delta H_{ads} = 0.38$ and 0.35 eV/C for (100) and (111)

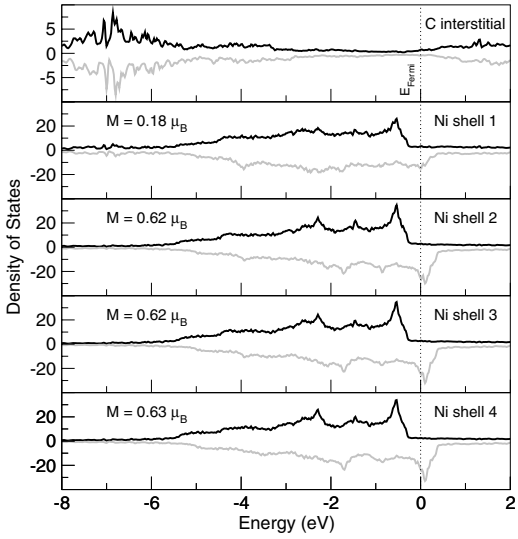

FIG. 1. Spin-polarized density of states (DOS) and average magnetic moments (M) for the Ni-C system, calculated using a supercell consisting of 128 Ni atoms and one C interstitial. Black curve: majority spin DOS; grey curve: minority spin DOS. Top panel: Total DOS for the C interstitial. Lower panels: partial (*d*-electron) DOS and magnetic moments for successive (farther) Ni neighbor shells around the C. Shell 1 consists of the six octahedral nearest-neighbor Ni atoms, and shell 4 is representative of elemental Ni.

surfaces at a C coverage of one quarter of a monolayer [20]. This is consistent with the notion that the surface adsorption sites have a lower coordination than bulk sites, and are therefore expected to suppress magnetism to a lesser extent. Since the primary effect of larger C coverages or other surface contamination is to reduce the magnitude of $\delta\Delta H_{\mathrm{ads}}$, it is expected that $\delta\Delta H_{\mathrm{seg}}$ will be dominated by $\delta\Delta H_{\mathrm{sol}}$ in all cases.

Next we present a more quantitative assessment of magnetism's impact upon impurity solubility. In order to model the temperature-dependent solubility, it is necessary to go beyond the limiting cases of perfectly ferromagnetic ($T \approx 0$ K) and paramagnetic ($T \gg T_C$) nickel, and calculate $\delta\Delta H_{\mathrm{sol}}$ for a range of temperatures spanning T_C. To accomplish this, we have employed a linear-response technique [17] to map the LSDA Hamiltonian onto a Heisenberg form:

$$H^J(\{s_i\}) = -\sum_{i,j} J_{i,j} s_i \cdot s_j, \tag{3}$$

which describes the energy as a function of the orientations of the local magnetic moments (s_i). The exchange coefficients ($J_{i,j}$) were obtained from two separate LSDA calculations (32 atom Ni and 33 atom Ni-C supercell), and used in a pair of spin-dynamics simulations on enlarged supercells of pure Ni (1728 atoms) and Ni-C (1728 Ni atoms + 54 C atoms). The spin-dynamics simulations give time dependent values for the fluctuating $s_i(t)$. The magnetic energy is calculated from the time average of the Heisenberg Hamiltonian [21]. It is well known for Ni that spin-dynamics calculations underestimate the value of T_C, with $T_C^{\mathrm{calc}} \approx 406$ K and $T_C^{\mathrm{expt}} \approx 627$ K [22]. To allow for this error, we rescale the theoretical temperature axis by $T_C^{\mathrm{expt}}/T_C^{\mathrm{calc}}$.

One way to check the validity of the Heisenberg Hamiltonian is to compare its prediction for the total magnetic energy, $E^J(T=\infty) - E^J(T=0) = \sum_{ij} J_{ij}$, to the LSDA magnetization energy, $E^{\mathrm{LSDA}}(\mathrm{PM}) - E^{\mathrm{LSDA}}(\mathrm{FM})$. For elemental Ni, our calculated $\sum_{ij} J_{ij}$ is 49 meV per Ni atom. This agrees well with our calculated LSDA value of 47 meV, considering that these two formulas represent radically different approaches to estimate the magnetic energy. Assuming the LSDA generates a reasonable value for the magnetic energy, the Heisenberg Hamiltonian will also, in spite of the fact that T_C is underestimated.

Figure 2 (top panel) shows the temperature-dependent magnetic energy calculated from the spin-dynamics calculations for pure Ni and for Ni-C. The curves show that the Curie point for Ni-C is substantially lower than that of elemental Ni, consistent with the quenching of Ni magnetic moments by C. Subtracting the two curves and multiplying by the Ni/C ratio gives the magnetic contribution to ΔH_{sol} (Fig. 2, bottom panel); there is a large increase in ΔH_{sol} as the temperature falls below T_C.

In Fig. 3 we use our calculated magnetic contribution to ΔH_{sol} to extrapolate experimental high-temperature Ni-C solubility data [13] to temperatures below T_C. Above the Curie point we fit the experimental data by a standard Arrhenius form:

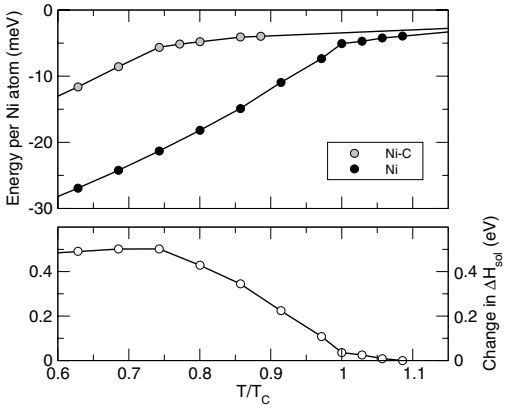

FIG. 2. Magnetization energy per Ni atom and magnetic contribution to ΔH_{sol} (per C atom) as a function of temperature. Top panel: Comparison of magnetization energies for elemental Ni (black circles) and Ni-C (grey circles) calculated from spin-dynamics simulations. The supercell for elemental Ni consists of 1728 atoms. The Ni-C supercell contains the same number of Ni atoms, with the addition of an ordered ~3 at. % array of C interstitials in octahedral sites. Bottom panel: Magnetic contribution to ΔH_{sol} obtained by taking differences between the Ni and Ni-C curves from the top panel. For larger, more realistic supercells, the transition is expected to be sharper.

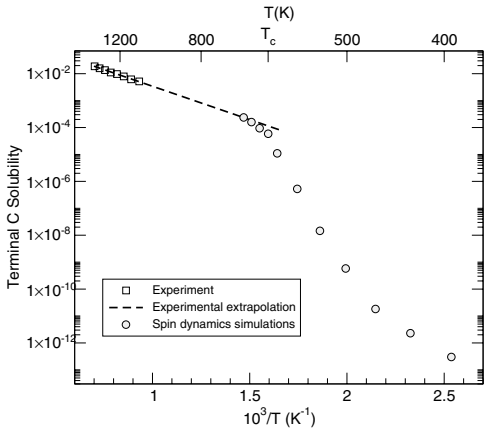

FIG. 3. Solubility of C impurities in Ni as a function of temperature. High temperature experimental data (squares) are taken from Ref. [13], and are fit (dashed line) to an Arrhenius form [Eq. (4)]. The low-temperature solubility (circles) was evaluated by adding the magnetic contribution to the heat of solution ($\delta\Delta H_{\mathrm{sol}}$, bottom panel of Fig. 2), calculated from spin-dynamics simulations, to the high-temperature, experimental ΔH_{sol}.

$$X_B = X_0 \exp[-\Delta H_{\mathrm{sol}}(\mathrm{PM})/k_B T], \tag{4}$$

where X_B is the bulk solubility, X_O is the (experimentally determined) solubility prefactor, and $\Delta H_{\mathrm{sol}}(\mathrm{PM})$ is the (experimentally determined) heat of solution at high temperature. For lower temperatures we extrapolate using the change in the heat of solution from the spin-dynamics calculation as follows:

$$X_B = X_0 \exp\{-[\Delta H_{\mathrm{sol}}(\mathrm{PM}) + \delta\Delta H_{\mathrm{sol}}(T)]/k_B T\}. \tag{5}$$

We see that the C solubility drops dramatically below the Curie point, providing the impetus for increased surface segregation.

In summary, we have calculated from first principles a sharp decrease in the solubility of C impurities in Ni for temperatures below the Curie point. The decreased solubility can be attributed to an increase in the heat of solution arising from carbon's (energetically unfavorable) suppression of ferromagnetism on adjacent Ni atoms. Our results are consistent with experimental observations of increased carbon surface segregation on nickel surfaces [3,5] below T_C, and with several reports of reduced impurity solubility in magnetic materials below the Curie point [7,13]. Our calculations explain these effects for the first time. They also explain many of the observations of the magnetocatalytic Hedvall effect, thereby solving a long-standing scientific puzzle bringing together the disciplines of chemistry, physics, and materials science.

This work was supported by the U.S. Department of Energy, Office of Basic Energy Sciences, Division of Materials Science, under Contract No. DE-AC04-94AL85000. We acknowledge helpful discussions with Norman Bartelt and Roland Stumpf.

*Corresponding author.
Email address: djsiege@sandia.gov

[1] M. S. Dresselhaus, Nature (London) **292**, 196 (1981).
[2] J. A. Hedvall, R. Hedin, and O. Persson, Z. Phys. Chem. Abt. B **27**, 196 (1934).
[3] H. Robota, W. Vielhaber, and G. Ertl, Surf. Sci. **136**, 111 (1984).
[4] G. Ertl, Surf. Sci. **152**, 328 (1985).
[5] J. C. Hamilton and T. Jach, Phys. Rev. Lett. **46**, 745 (1981).
[6] H. V. Thapliyal and J. M. Blakely, J. Vac. Sci. Technol. **15**, 600 (1978).
[7] K. Zeng, T. Klassen, W. Oelerich, and R. Bormann, J. Alloys Compd. **283**, 151 (1999).
[8] J.-Z. Yu, Q. Sun, Q. Wang, U. Onose, Y. Akiyama, and Y. Kawazoe, Mater. Trans., JIM **41**, 621 (2000).
[9] H. J. Zeiger, B. Wasserman, M. S. Dresselhaus, and G. Dresselhaus, Phys. Rev. B **28**, 317 (1983).
[10] M. P. Kiskinova, Surf. Sci. Rep. **8**, 359 (1988).
[11] E. I. Ko and R. J. Madix, Appl. Surf. Sci. **3**, 236 (1979).
[12] C. H. Bartholomew, Appl. Catal. A **212**, 17 (2001).
[13] M. Hasebe, H. Ohtani, and T. Nishizawa, Metall. Trans. A **16**, 913 (1985).
[14] S. Diamond and C. Wert, Trans. Metall. Soc. AIME **239**, 705 (1967). (There is no anomaly in D at T_C.)
[15] P. Hohenberg and W. Kohn, Phys. Rev. **136**, B864 (1964).
[16] M. Methfessel, M. van Schilfgaarde, and R. A. Casali, *Electronic Structure and Physical Properties of Solids: The Uses of the LMTO Method* (Springer-Verlag, Berlin, 2000), p. 114.
[17] M. van Schilfgaarde and V. P. Antropov, J. Appl. Phys. **85**, 4827 (1999).
[18] W. Kohn and L. J. Sham, Phys. Rev. **140**, A1133 (1965).
[19] Tests performed on a 109-atom supercell ($\delta\Delta H_{\mathrm{sol}} = 0.51$ eV) revealed that our results for the 33-atom cell ($\delta\Delta H_{\mathrm{sol}} = 0.48$ eV) were well converged with respect to system size. Errors due to finite **k**-point sampling were determined to be within 0.02 eV. Basis set effects were examined by comparing results obtained with a plane-wave pseudopotential method, a full-potential LMTO method, and an LMTO-atomic sphere approximation method: All three methods were found to be in good mutual agreement. Use of a gradient-corrected exchange-correlation functional also yielded similar results.
[20] To accurately compare the relative magnitudes of $\delta\Delta H_{\mathrm{ads}}$ and $\delta\Delta H_{\mathrm{sol}}$, we reevaluated $\delta\Delta H_{\mathrm{sol}}$ within the same (111) and (100) surface supercells, and with the same computational parameters, as used to determine $\delta\Delta H_{\mathrm{ads}}$. In this case the C atom was placed at an octahedral (bulklike) site near the center of the slab. We find $\delta\Delta H_{\mathrm{sol}} = 0.51$ and 0.54 eV for the (100) and (111) supercells, respectively.
[21] V. P. Antropov *et al.*, Phys. Rev. B **54**, 1019 (1996).
[22] Antropov has found [23] that the LSDA reasonably well describes Ni near T_C, but for various reasons the corrections to the linear response of Ref. [17] are sizable for Ni. A dynamical mean-field treatment [24] suggests that the amplitude of the local moment for $T > T_C$ is partially quenched, but fluctuates in time.
[23] V. P. Antropov, J. Magn. Magn. Mater. **262**, L192 (2003).
[24] A. I. Lichtenstein, M. I. Katsnelson, and G. Kotliar, Phys. Rev. Lett. **87**, 067205 (2001).